Journal of Electrochemistry

Volume 20
Issue 3 *Special Issue on Fundamental Electrochemistry(Editor: Professor CHEN Sheng-li)*

2014-06-28

Effects of Conformational Transformations on Electronic Transport Properties of Optical Molecular Switches: An ab initio Study

Yuan-yuan HE

Jian-wei ZHAO
State Key Laboratory of Analytical Chemistry for Life Science, School of Chemistry and Chemical Engineering, Nanjing University, Nanjing 210008, China;, zhaojw@nju.edu.cn

DOI: 10.13208/j.electrochem.130881 **Artical ID**:1006-3471(2014)03-0243-17
Cite this: *J. Electrochem.* **2014**, *20*(3): 243-259 **Http**://electrochem.xmu.edu.cn

Effects of Conformational Transformations on Electronic Transport Properties of Optical Molecular Switches: An *ab initio* Study

HE Yuan-yuan, ZHAO Jian-wei*
(*State Key Laboratory of Analytical Chemistry for Life Science, School of Chemistry and Chemical Engineering, Nanjing University, Nanjing* 210008, *China*)

Abstract: A series of model molecules with 4 kinds of conformational transformations have been investigated as optical molecular switches by using density functional theory combined with nonequilibrium Green's function method. The theoretical calculations show that molecules after conformational transformations have photoswitching characteristics. We find that the photochromic molecules with the same conformational transformation usually have a similar current on/off state when they are applied as photoshwitches. Among these transformations, the molecular switch with *E*("*trans*")/*Z*("*cis*")-isomerisation of the N=N double bond has the highest current on-off ratio. The influences of the energy gap (HLG) between the highest occupied molecular orbital (HOMO) and the lowest unoccupied molecular orbital (LUMO), spatial distributions, transmission and projected density of states (PDOS) spectra on the electronic transport through the optical molecular switches are discussed in detail.

Key words: conformational transformation; photochrome; electronic transport; current on-off ratio; molecular orbitals

CLC Number: O621.13; O561 **Document Code:** A

Photochromic molecules that change color upon irradiation with ultraviolet (UV) light or visible (VIS) light have attracted much attention because of their possible applications in optical molecular switches and devices[1-4] (Scheme 1). In recent years, most mechanisms for optical switches are based on light-induced conformational changes, in particular *cis-trans* isomerization reactions or ring-opening reactions of the molecular bridge, ring-closing reactions of the merocyanine and internal conversion[5-7].

Profiting from the recent progress in experimental techniques for characterizing and manipulating in-

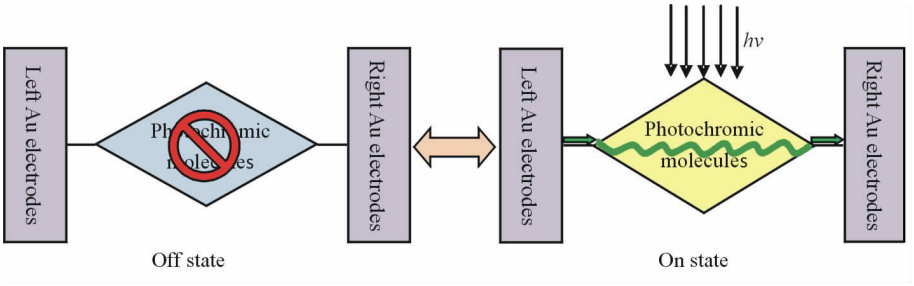

Scheme 1 The schematic representation of the photochromism process in optical molecular switch system (the molecule transforms between current on and off states)

Received: 2013-08-08, Revised: 2013-11-05 *Corresponding author, Tel: (86-25)83596523, E-mail: zhaojw@nju.edu.cn
This work was supported by National Natural Science Foundation of China (Nos. 51071084, 21273113, 21121091 and 11204120) and National Key Technology R&D Program of China (No. 2012BAF03B05)

dividual molecules, many characteristics of photochromic molecules have been measured during the past decade, such as current/voltage characteristics[8], photochemical fatigue[9], light wavelengths, attainable conversion efficiencies [10], and so on. Interested in the superior photoswitching characteristics of photochromic compounds, many researches have focused on new types of optical molecular switches. For example, Coelho have synthesized a series of novel pyrrolidene imines bearing functionalized aryl or naphthyl moieties and studied their photochromic properties by UV spectroscopy, which proved that molecule with trans-cis photoisomerization of the N═N double bond has good photoswitching characteristics[11]. Diana Dulic group synthesized a 1,2-bis [5′- (5″-acetylsulfanylthien-2′ -yl)-2′ -methylthien-3′ -yl] cyclopentene photochromic switch and used the mechanically controllable break-junction technique (MCBJ) to measure electronic transport and UV/VIS spectroscopy to measure absorption, which reflected the potential application of molecules with ring-opening reactions in optical molecular switches[12]. Helge Schenderlein prepared surface-attached polymer networks that carry light-responsive nitrospiropyran groups in a hydrophilic PDMAA matrix on planar silicon and glass surfaces and characterized them with respect to their switching behavior under the influence of an external light trigger, which also is based on the photoswitching characteristic of molecules with ring-closing reactions of the merocyanine[13]. Zhao fully encapsulated multiresponse molecule salicylidene Schiff base, N-3, 5-dichlorosalicylidene-(*S*)-*R*-phenylethylamine (SPEA) into the channel of amino-functionalized mesoporous molecular sieve and characterized its photoswitching properties by X-ray diffraction, Fourier transform infrared spectroscopy, transmission electron microscopy, UV-VIS diffuse reflectance spectroscopy, and photoluminescence spectroscopy[14].

When these model molecules with 4 kinds of conformational transformation are applied as molecular switches, many theoretical studies have described their own characteristics. The switchable behavior of the series of spiropyran derivatives has been confirmed according to their time-dependent Hatree-Fock (TDHF), coupled perturbed (CP) HF, and Moller-Plesset (MP2) calculations[15]. Computed vertical-absorption spectra for the stable ground-state isomers of salicylidene methylamine (SMA) fully confirm the photochromism of SMA. The photophysical scheme which emerges from the theoretical study is related to recent experimental results obtained for SMA and its derivatives in the low-temperature argon matrices[16-17]. A detailed comparison of the S_0, S_1 (n -> pi*) and S_2 (pi -> pi*) potential energy surfaces (PESs) of the prototypical molecular switch azobenzene is obtained by Delta-self-consistent-field (Delta SCF) density-functional theory (DFT), time-dependent DFT (TD-DFT) and approximate coupled cluster singles and doubles (RI-CC2). All three methods unanimously agree in terms of the PES topologies, which are furthermore fully consistent with existing experimental data concerning the photo-isomerization mechanism[18-19]. The multi-switchable molecular systems incorporate at least one diarylethene group which is the most successful thermally stable (*P*-type) organic photochrome. The promising successes of asymmetric diarylethene dimmers, trimers, and molecules combine two families of photochromes, such as diarylethene added to fulgimide or phenoxynaphthacenequinone. The investigation of the absorption spectra of the photochromes with time-dependent density functional theory (TD-DFT), the analysis of the topology of the LUMO + n (typically n = 1) of the closed-open hybrid, and an estimation of the steric stress in the hypothetical (ground-state) closed-closed structure serve as a useful combination of parameters to obtain initial insights regarding the photocydization of the different open diarylethene groups[20]. Although many efforts have been made for improving the photoswitching characteristics of photochromic compounds and the applicable theoretical explanation to these characteristics, it still hasn't been compared between different conformational transformations under the same conditions, thus it is not yet clear that what kind of compound is most applicable in optical molecular switch.

We focus on the first principles theoretical investigation of the electron transport behavior for a series of photochromic molecules most widely studied in the application of photochromes, which have been included by the 4 kinds of chemical transformations under photoexcitation mentioned above. By comparison, we find that electron transfer can affect the molecular conductance and current significantly as shown in the electron distribution of the molecules. The main aim of this study is to theoretically investigate the static and dynamic features of current on/off states for photochromic molecular switches, such as the molecular projected self-consistent Hamiltonian (MPSH) orbitals, transmission spectra and the projected density of states (PDOS) spectra, and to further understand their switching behavior in detail. Thus, it can provide a useful candidate to design molecular switch.

1 Methodology

1.1 The Model Systems

Fig. 1 depicts the photoisomerisation reactions of several important classes of photochromic switches, namely (A) spiropyranes, spirooxazines; (B) salicylidene schiff bases, phenanthrenequinones; (C) azobenzenes, dihydrodibenzodiazocines; (D) fulgimides and diarylethenes. They are the core functional molecules that most researchers synthesize and study in photochromes field [21-24]. The respective conformational transformations include (A) electrocyclic ring opening to the merocyanine form (spirobenzopyrans and spirooxazines); (B) internal conversion (salicylidene schiff bases and phenanthrenequinones); (C) *E*/*Z*-isomerisation of the N═N double bond (azobenzenes and diazocines) and (D) electrocyclic ring closure of the hexatriene backbone to cyclohexadiene (fulgimides and diarylethenes). The molecular junctions are shown in Fig. 1, giving the sequential series of photoswitching units in on and off states. Each model has two thiol groups on the opposite position of the junction to attach onto the left and the right electrodes, or the drain and the source electrodes.

1.2 Computational Method

All the electronic structure calculations are carried out using DFT[29], as implemented in the Gaussian-03 software package[30]. A combination of Becke's three-parameter (B3)[31] exchange functional and Lee, Yang and Parr (LYP) gradient-corrected correlation functional i.e., B3LYP hybrid functional is used for the entire calculations. Thus, this hybrid method gives values that are in close agreement with the experimental data[32]. The LANL2DZ basis set is used for the DFT calculation, in which LANL (Los Alamos National Laboratory) provides effective core potential (ECP)[33-34] for heavy atoms (Au and S atoms) and the double zeta (DZ) type basis set D95V[35] is utilized as valence basis set. The use of ECP for the core electrons simplifies the problem by eliminating the need for the core basis functions, which requires large computation, at the same time the accuracy is also maintained.

Fig. 1 illustrates the simulation setup. The pre-optimized molecules are sandwiched via thiolate bonds between two parallel Au (111) surfaces that correspond to the surface of the Au electrode[36-37]. Sulfur atoms are always chemisorbed at the center of the centers of the triangles, namely, the hollow site which is energetically favorable for providing a good electrical contact between the organic molecule and the metal electrode. The relative position of Au atoms is frozen in each triangle cluster, but the distance between the Au clusters is relaxed during the process of further geometric optimization at the same level of theory. Each layer of gold electrodes is represented by a 3×3 supercell with the periodic boundary condition so that it imitates bulk metal structures[38-39]. Photoswitching molecule is rotated to an appropriate position to make sure that the 3×3 supercell is large enough to avoid any interaction with molecules in the next supercell[40-41]. In NEGF theory, the entire molecular switch is divided into three regions: left electrode (L), contact region (C) and right electrode (R). The contact region includes extended molecule and two layers of gold slab from each electrode to screen the perturbation effect from the central region and they are denoted as surface-atomic layers. The semi-infinite electrodes are calculated separately to obtain the

A. Electrocyclic ring opening to the merocyanine form[25]

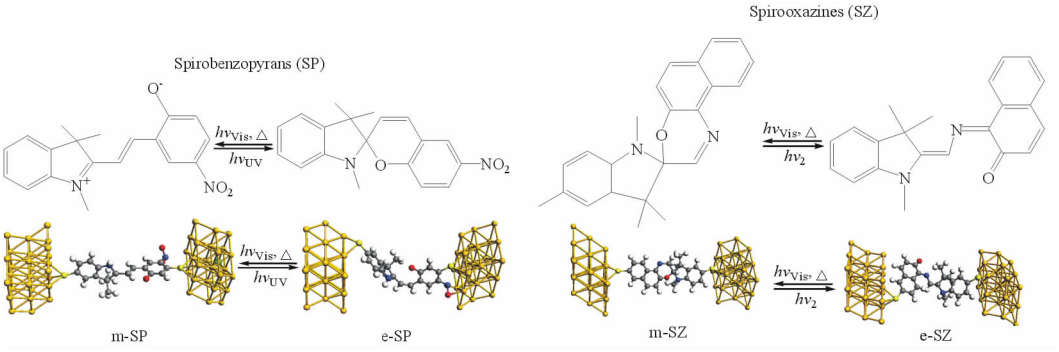

B. Internal conversion[26]

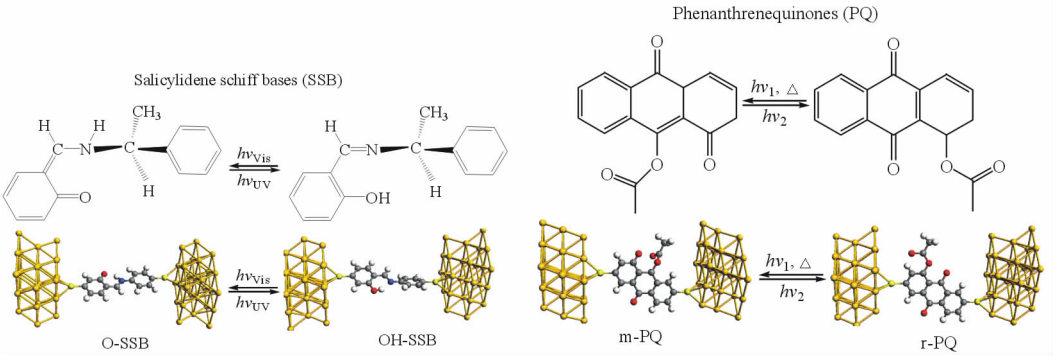

C. *E*/*Z*-isomerisation of the NN double bond[27]

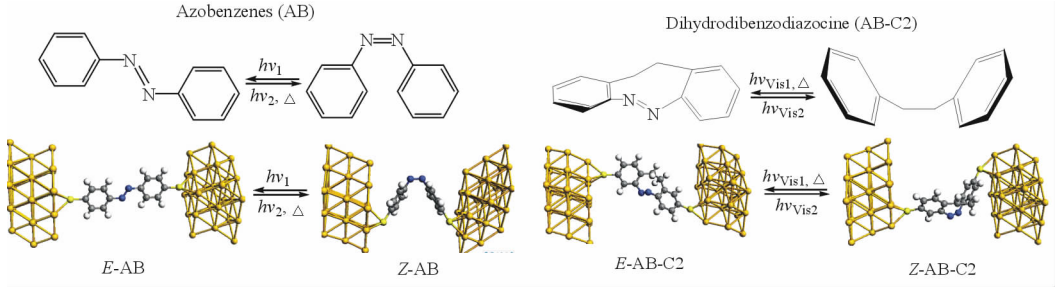

D. Electrocyclic ring closure of the hexatriene backbone to cyclohexadiene[28]

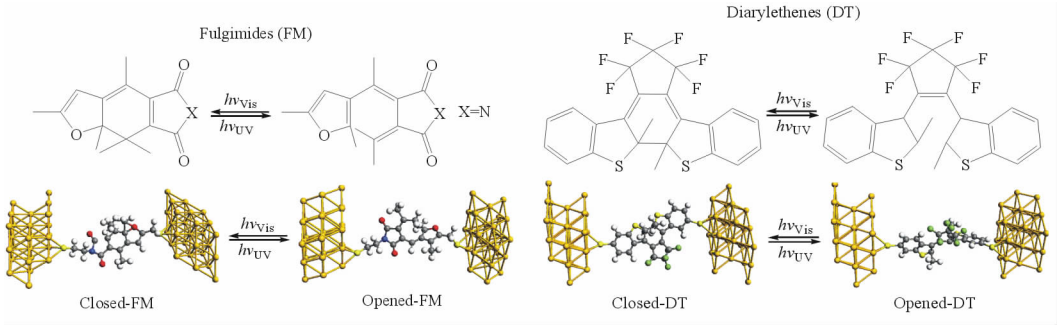

Fig. 1　The photoswitching units can convert between a circuit-on and off configuration upon photoexcitation　(all the models sandwiched between two Au(111) nanoscale electrodes with finite cross section)

bulk self-energy. The geometry of the central extended molecule is optimized by minimizing the atomic forces on the photoswitching molecule to be smaller than 1 eV·nm^{-1}. This optimization and further quantum transport calculation are based on the real-space, Keldysh NEGF formalism and the density functional

theory (DFT) as implemented in the Atomistix Toolkit (ATK) software[42].

In the molecule geometrical optimization and the electronic transport properties of the molecular switch, the double-ζ plus polarization (DZP) basic set for the organic and a single-ζ plus polarization (SZP) basis set for gold atoms are adopted. The molecule-electrode contact distance was initially set as 0.2 nm and then optimized. The reasonable range is from 0.190 to 0.239 nm that is used by most authors[43-45]. The exchange-correlation potential was described by the PBE parameterization of generalized-gradient approximation (GGA) function[46-47]. An energy cutoff of 150 Ry for the grid integration is set to present the accurate charge density.

In NEGF theory, the transmission function $T(E, V)$ of the system is the sum of transmission probabilities of all channels available at energy E under external bias V[48]:

$$T(E,V)=Tr[\Gamma_{L}(E,V)G^{R}(E,V)\Gamma_{R}(E,V)G^{A}(E,V)] \quad (1)$$

where $G^{R/A}$ are the retarded and advanced Green's functions, and coupling functions $\Gamma_{L/R}$ are the imaginary parts of the left and right self-energies, respectively. The self-energy depends on the surface Green's functions of the electrode regions and comes from the nearest-neighbor interaction between the extended molecule region and the electrodes.

For the system at equilibrium, the conductance G is evaluated by the transmission function $T(E)$ at the Fermi level E_F of the system[48]:

$$G = G_0T(E_F) \quad (2)$$

Where $G_0 = 2e^2/h$ is the quantum unit of conductance, h the Planck's constant, and e is the electron charge.

2 Results and Discussion

2.1 Spirobenzopyran and Spirooxazines

1) Electron Transport properties

Spirobenzopyrans (SPs) and spirooxazines (SZs) are the typical photochromes by electrocyclic ring opening to the merocyanine form upon photoexcitation. These properties derive from the photochromism of SPs upon ultraviolet excitation, which converts the closed, colorless form (electrocyclic ring, e-SP) to an open colored form (merocyanine, m-SP). The m-SP may be thermally converted back to e-SP. The m-SZ is similar to m-SP and easily converted to the ring-opened form (e-SZ) upon UV irradiation, and has excellent fatigue-resistance property to light[49]. Therefore, SPs and SZs are considered suitable materials for technological applications like optical memory devices and switches, as well as models for biological receptors.

The currents as a function of junction bias from 0 to 1.0 V are presented in Fig. 2A. One can see that the current through e-SP is strongly suppressed over the entire bias range and the current through m-SP is evidently larger than that through e-SP. Thus, when e-SP changes to m-SP under photoexcitation, it is predicted to switch from a weakly conducting (off state) to a highly conducting state (on state), and vice versa. The switch status for SZs is similar to that of SPs, in which m-SZ is on state and e-SZ is off state. In addition, the current of m-SZ (on state) is nearly two times higher than that of m-SP (on state). However, the on-off ratio in the current of SPs, $R(\mathrm{V}) = I_{on}/I_{off}$, is much higher than that of SZs, which attributes to the higher current through e-SZ than that through e-SP. Although the ratio difference between SPs and SZs, their evolutions versus bias (V) are quite similar (Fig. 2A) in that they both generally decrease as bias rises.

The conductance-bias curves of all junctions of SPs and SZs are presented in Fig. 2B. The conductance changes of m-SP and e-SP have a similar tendency that they both rise up to a peak value and then decline slightly. However, the conductance of m-SZ declines, while that of e-SZ increases when the bias further rises. This phenomenon can be explained by the following MPSH orbital energy.

2) HOMO, LUMO, and Energy Gap between HOMO and LUMO

The current through a single molecule that bridges two metal electrodes is given by the Landauer-Büttiker formula[50-51],

$$I=\frac{2e}{h}\int_{-\infty}^{+\infty}\{T(E,V_b)[f_L(E-\mu_L)-f_R(E-\mu_R)]\}dE \quad (3)$$

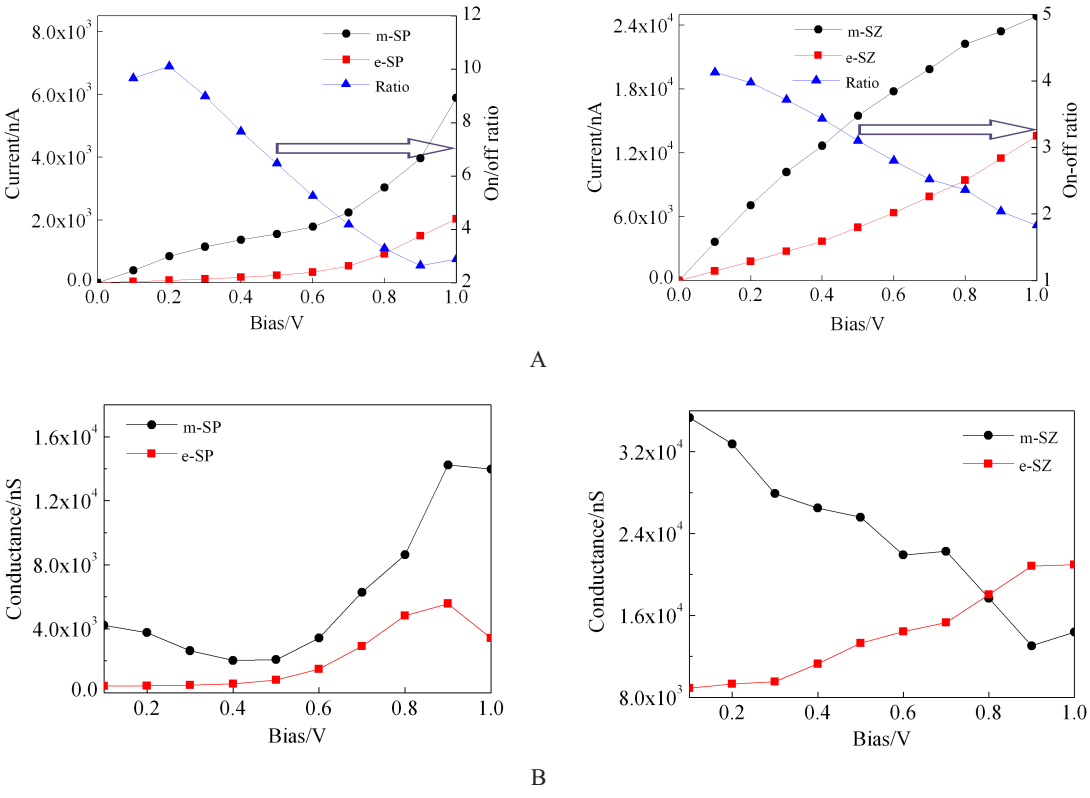

Fig. 2 A. The *I*-*V* and on-off ratio curves as function of the bias; B. The conductance-bias curves of SPs and SZs with all junctions (the bias changes from 0.0 V to 1.0 V)

where $T(E,V_b)$ is the transmission probability at a given bias voltage V_b, $f_{L/R}$ is the Fermi-Dirac distribution function for the left(L)/right(R) electrode, and $\mu_{L/R}$ is the electrochemical potential of the L/R electrode. The bias window is given by $\mu_L = E_F - eV_b/2$ and $\mu_R = E_F + eV_b/2$, in which E_F is the Fermi energy that can be referred to zero. $[\mu_L(V_b), \mu_R(V_b)]$ is the energy region that contributes to the current integral and is referred to as the bias window.

The levels of frontier molecular orbitals (FMOs) are shown in Fig. 3. The Fermi level of the gold electrode is set at zero and HOMO corresponds to the energy levels with the highest energy under zero while LUMO corresponds to the energy levels with the lowest energy over zero. Though they may not correspond to the insulated molecule, they are an important factor dominating the junction transportation. It can be expected that only electrons with energies around the Fermi level contribute to the total current. To take SPs for example (Fig. 3A), since the HOMO level of e-SP and the LUMO level of m-SP are closer to the Fermi level compared to the LUMO level of m-SP and e-SP at a wide bias range, the HOMO level of e-SP and the LUMO level of m-SP mainly contribute to their current. When SZs are applied as photochromes, the HOMO and LUMO levels of m-SZ are out of the bias window in the entire bias range but the LUMO level of e-SZ is in the bias window when the bias is up to 0.7 V, thus the LUMO level of e-SZ contributes to its conductance. As a result, the conductance of e-SZ is larger than that of m-SZ when the bias is higher than 0.7 V, thus the HOMO resonance forms the main electron transport channel. When the applied bias increases, both the HOMO and LUMO levels of e-SZ go up whereas the HOMO and LUMO levels of m-SZ drop down. We further analyze the MPSH level through the bias window which is defined as the energy range from $-(V_b/2)$ to $(V_b/2)$. The HOMO and LUMO levels of m-SZ are both located in the bias window at high bias ($\geqslant$ 0.7 V) but only

the HOMO level of e-SZ is in, thus, the LUMO level of m-SP also contributes to its current. Hence, the current of m-SP is larger than that of e-SP. In contrast, only the HOMO level of m-SZ is located in the bias window. The conductance of e-SZ is higher than that of m-SZ.

The parameter HLG is the gap between the energy level of the highest occupied molecular orbital (HOMO) and the lowest unoccupied molecular orbital (LUMO) of the molecule. HLG and the conjugation structure of FMOs are critical parameters in determining molecular electron transport properties. In most cases, the electron transport barrier is directly correlated to the HLG. Because the drop of HLG can make it easier for electron to jump from HOMO orbital to LUMO orbital, it may give insight into understanding many electron-transfer behaviors of the molecular wire, and further facilitate the design of the novel molecular electronic devices. When other factors keep the same, the conductance is proportional to the HLG[52-53]. The HLG as a function of bias is presented in Fig. 3B. The HLG of m-SP is greatly lower than that of e-SP. Hence, it is easier for elec trons to go through m-SP. Although the HLG of m-SZ is also lower than that of e-SZ, since the HOMO and LUMO levels of m-SZ are both out of the bias window, the less HLG of m-SZ has no contribution to its conductance. Therefore, the HLG curves of SZs are not used to explain the conductance difference of SZs with different junctions.

As demonstrated by us and others, the spatial distribution of the FMOs is a good indicator of molecular electron transfer, which not only qualitatively shows whether these orbitals form the transport channels, but also describes the coupling between the molecule and the electrode. The higher delocalization

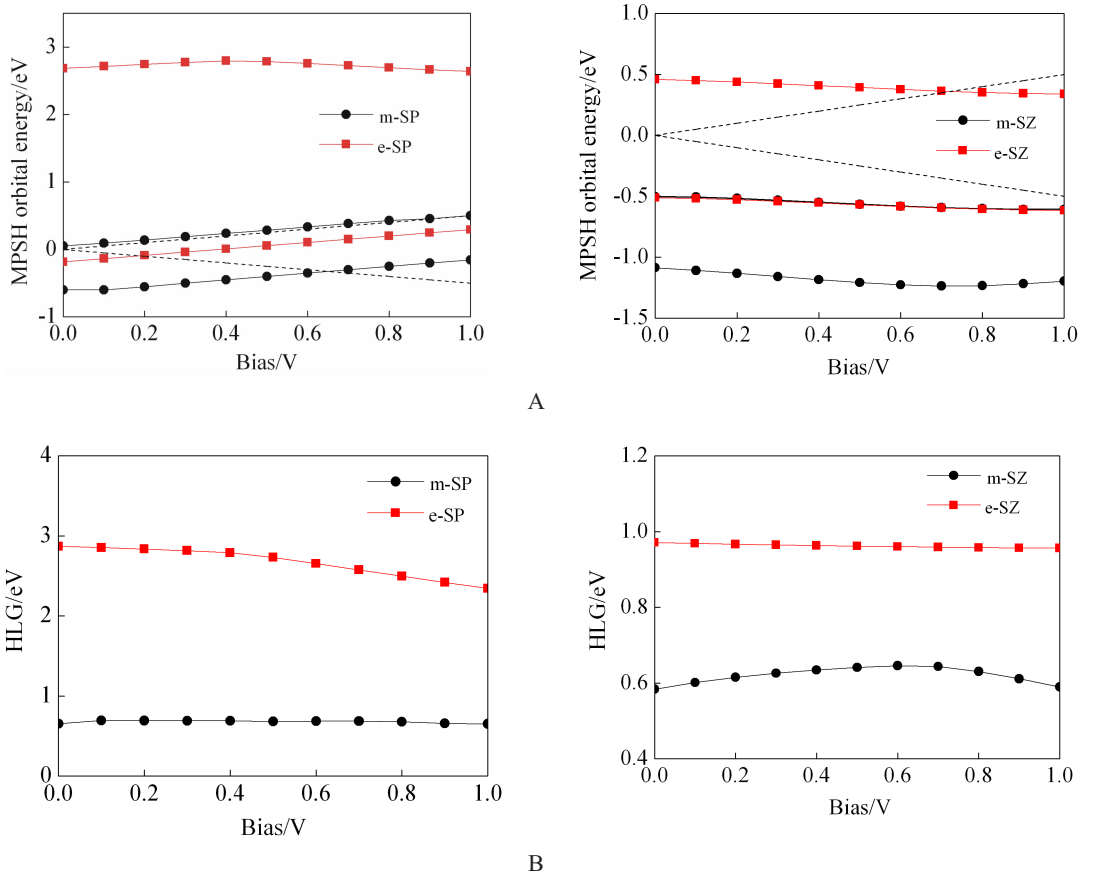

Fig. 3　A. The HOMO and LUMO levels of SPs and SZs with all junctions　(the region between the dash lines stands for the bias window); B. The HLG dependence on external bias of SPs and SZs with all junctions

is the molecule, the easier is the electron transfer, and vice versa. The spatial distributions for the FMOs of SPs and SZs with different junctions are presented in Fig. 4. The results are calculated by ATK software at the bias of 1.0 V. For m-SP and m-SZ, the HOMO levels are both much more delocalized than those of e-SP and e-SZ, and the spatial distributions of their HOMO-1 and LUMO+1 channels overlap with Au electrode greatly. Therefore, the higher currents of m-SP and m-SZ benefit from the delocalized FMOs. The spatial distribution results further proved the current and conductance differences between SPs and SZs with different junctions.

3) Transmission and PDOS Spectra

As current is the integral of the transmission coefficient in the bias window, the analysis of the transmission spectra may give us a clear understanding of the electron transport behavior. The transmission spectra of SPs and SZs at the bias of 1.0 V are plotted in Fig. 5. For e-SP, only the HOMO orbital is in the bias windows whereas both the HOMO and LUMO levels are in the bias windows for m-SP. The integral area of the peaks in the bias window of m-SP is also larger than that of e-SP, which illustrates that the current of m-SP is higher than that of e-SP. In the case of SZs, there is a strong HOMO peak for m-SZ in the bias window, whereas there is no peak for e-SZ. Therefore, the photoswitching unit with m-SZ is in current on state.

Furthermore, PDOS spectra of SPs and SZs can give insights into the states contributing to molecular switching. Fig. 5 plots PDOS spectra of these two photochromes at 1.0 V. In the case of e-SP (Fig. 5A), two resonance peaks are observed at -0.4 and 0.5 V, originating from the HOMO and LUMO states, respectively. The resonance peaks of m-SP are at -0.3 and 0.4 V, and are originated from the HOMO and LUMO of m-SP. The HOMO and LUMO resonances of m-SP are wider and closer to Fermi level compared to that of e-SP, which is consistent to the transmission of SPs. Similar phenomenon can also be observed in the PDOS spectra of SZs. The conclusions can be initially drawn that the photochromic molecules with the same structural transformation usually have a similar current on/off state when they are applied as photoshwitches.

2.2 Salicylidene Schiff Bases and Phenanthrenequinones

1) Electron Transport Properties

Salicylidene schiff bases (SSBs) and phenan threnequinones (PQs) are the typical photoswitching units by internal conversion upon photoexcitation. After photoexcitation, in SSB molecule, the position of a hydrogen atom has transferred from the nitrogenous group onto the phenyloxy group whereas the position of carbonyl group is transferred from phenyloxy group on the middle benzene ring to phenyloxy group on the right benzene ring in PQ molecule[54-55]. In Fig. 6A, we show the self-consistently calculated *I-V* characteristics curves of the two kinds of molecular switches with different forms in a bias range from 0 to 1.0 V. The current through SSB that hydrogen atom is on the nitrogenous group (O-SSB) almost linearly increases with the bias voltage, whereas the current curve of SSB that hydrogen atom is on the phenyloxy group (OH-SSB) has a higher slope in the

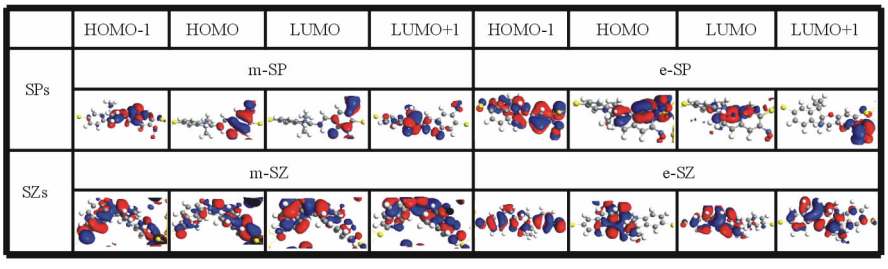

Fig. 4 Spatial distributions of HOMO-1, HOMO, LUMO and LUMO+1 at the bias of 1.0 V, including SPs and SZs with electrocyclic ring and merocyanine junctions

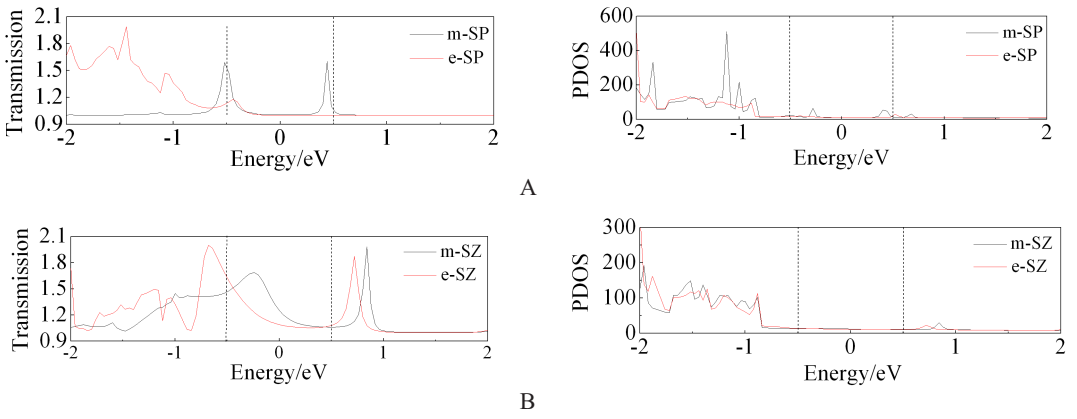

Fig. 5 Transmission and PDOS spectra for SPs (A) and SZs (B) at 1.0 V (the region between two dash lines means the bias window)

low bias and then the increasing speed slows down. The current through OH-SSB is apparently higher than that through O-SSB at low bias. Thus, one can predict that there is a switch from on (low resistance) state to the off (high resistance) state, when SSB molecule reverses from O-SSB to OH-SSB upon photoexitation. The current curves of PQs with different junctions are opposite to those through SSBs in that they have a small slope value in the low bias, and then increase rapidly with the bias after the bias is up to 0.5 V. Meanwhile, the current through the PQ that the carbonyl group is on phenyloxy group of the middle benzene ring (m-PQ) is evidently greater than that through the PQ that the carbonyl group is on phenyloxy group of the right benzene ring (r-PQ) over the entire bias range.

Based on the current evolutions below, the on-off current ratios of SSBs and PQs also show different trends (Fig. 6A). The ratio of SSB has a plat form when the bias is lower than 0.4 V and then decreases nearly linearly with the bias, while that of PQs first decreases and then increases at the bias of 0.3 V. The SSB switch has a max ratio value of 2.30 at 0.4 V and the PQ switch has a higher max value of 8.00 at 1.0 V. The average ratio of PQs is also much higher than that of SSBs, which would be attributed to the less current value of r-PQ. It can be concluded that the bias is an important factor that can affect the on/off ratio of a molecular switch.

The conductance-bias curves of all junctions of SSBs and PQs are also presented in Fig. 6B. Like the *I-V* curves, the conductance of O-SSB and r-PQ both increase by the bias increasing. There is extraordinary difference between the conductance curves of OH-SSBs and m-PQs, as the conductance of OH-SSB first increases and then decreases at 0.5 V, but the conductance of r-PQ first increases slowly and then accelerates the increasing rate at the same bias. The conductance of PQs is lower than that of SSBs at low bias. However, at the high bias, the conductance of PQs has exceeded that of SSBs for many times. The huge currents and conductance differences between all junctions of SSBs and PQs testifies the potential applications of SSBs and PQs in optical molecular switches.

2) Spatial Distributions of HOMO and LUMO Orbitals

Fig. 7 illustrates the spatial distributions of the HOMO-1, HOMO, LUMO and LUMO+1 at the bias of 1.0 V. The HOMO-1 and HOMO of OH-SSB are fully delocalized and provide a good channel for the electron transport. Meanwhile, the HOMO and LUMO of O-SSB also have a good delocalization despite not as good as that of OH-SSB, leading to the negligible HOMO and LUMO resonance peaks of OH-SSB and O-SSB as shown in Fig. S2. MPSH curves of PQs in Fig. S1 indicate that the electron transport of PQs in on state is mainly controlled by HOMO resonance of m-PQ as it is closer to Fermi level. The excellent spatial distribution in HOMO of

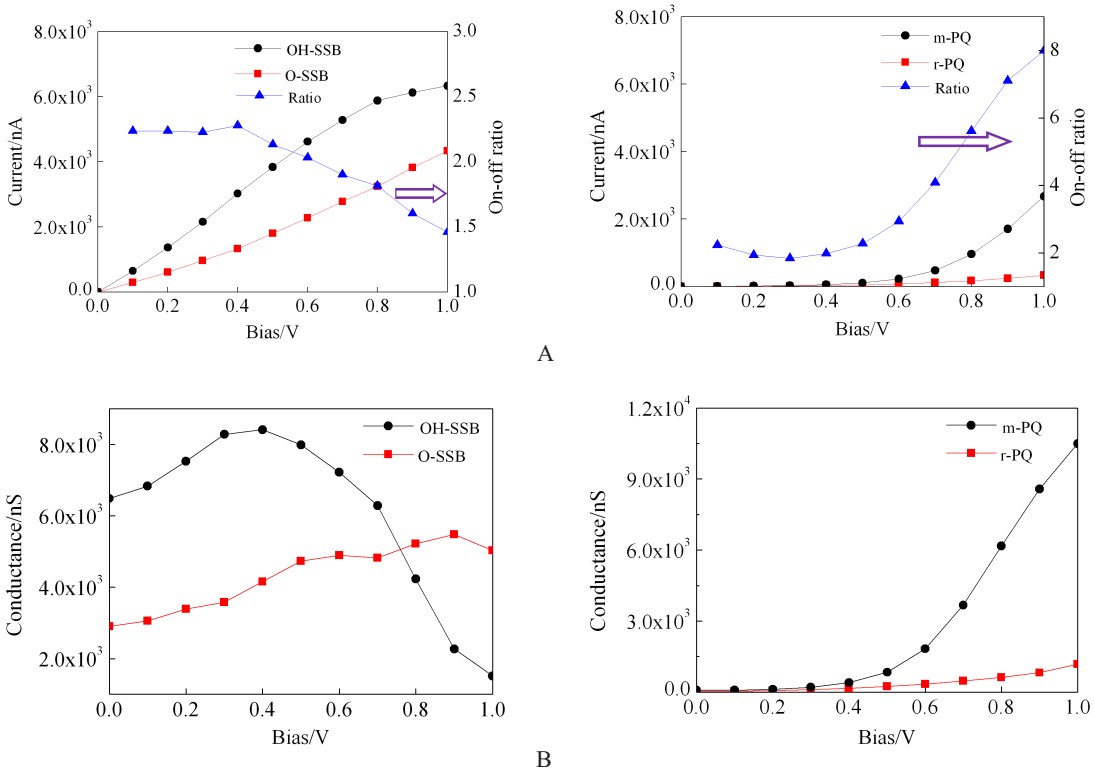

Fig. 6 A. The *I*-*V* and on-off ratio curves as function of the bias; B. The conductance-bias curves of SSBs and PQs with all junctions (the bias changes from 0.0 V to 1.0 V)

m-PQ shows that it provides the main electronic transport channel for m-PQ leading to low barrier for electron transport, which further supports the MPSH results.

As shown in Fig. S1, the current and conductance differences between OH-SSB and O-SSB can not be explained by the MPSH and HLG curves with the bias as the HOMO and LUMO levels are out of the region of bias window, which indicates that the total currents of SSBs with different junctions are not contributed by the HOMO and LUMO resonance. But in transmission spectra, as current is the integral of the transmission coefficient in bias window, the current of OH-SSB is still a little larger than that of O-SSB, thus the molecular switch with OH-SSB is in on state when the bias is 1.0 V (Fig. S2). However, in the PQs system, HLG of m-PQ is less than that of r-PQ, which results in a high conductance of m-PQ that is 2 ~ 3 orders of magnitude larger than that of r-PQ. And only the LUMO resonance peak of m-PQ

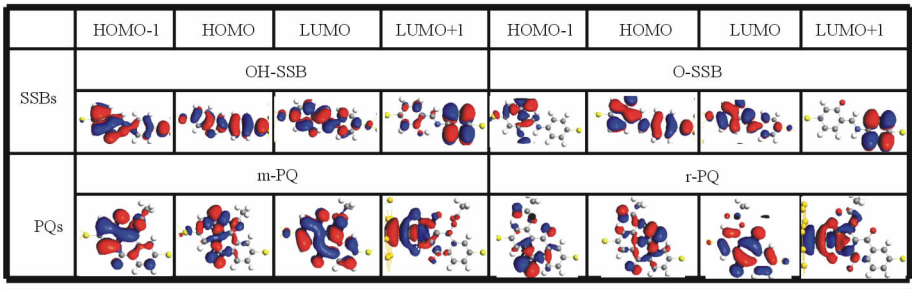

Fig. 7 Spatial distributions of HOMO-1, HOMO, LUMO and LUMO+1 at the bias of 1.0 V, including SSBs and PQs with all junctions

is in the bias window around the Fermi level in transmission and PDOS spectra, resulting in a high current and conductance of m-PQ.

2.3 Azobenzenes and Dihydrodibenzodiazocine

1) Electron Transport Properties

Azobenzenes (AB) and dihydrodibenzodiazocines (AB-C2) are the typical photoswitching units that are achieved by *E*("trans")/*Z*("cis")-isomerisation of the N═N double bond under photoexcitation. Azobenzene (AB) and its derivatives play particularly important roles in the field of photochromic molecular switches because of the large change in molecular size, shape and dipole moment from the thermodynamically favored, stretched *E* isomer to the energetically higher, more compact *Z* isomer, which can be interconverted through reversible *E*-*Z* and *Z*-*E* photoisomerisation reactions on irradiation with VIS or UV light. In addition, AB stands out for its low photochemical fatigue, which guarantees high numbers of switching cycles. For many applications, however, the photoswitching properties of AB are far from ide al. AB-C2, a bridge derivative of AB, has been synthesized recently in an effort to enhance the efficiency of the AB photochrome[56-58].

The calculated *I*-*V* curves of molecular switches with *E*/*Z* isomers of ABs and AB-C2s in the range of [0, 1.0 V] are plotted in Fig. 8A. The *I*-*V* curves of *E*/*Z* isomers of ABs are fairly linear in the entire voltage regime. This indicates that it is a simple tunneling for conduction electrons of the gold electrodes through the gap between the HOMO and LUMO orbitals. Meanwhile, the *I*-*V* curve of the E-isomer of AB-C2 (*E*-AB-C2) increases at first slowly and then rapidly but the current through *Z*-AB-C2 keeps a constant increasing slope in the entire bias range, as a result, the on/off state of *E*/*Z*-AB-C2 has been reversed at the bias of 0.4 V. By comparison, the current through *E*-AB is higher than that through *E*-AB-C2 but the current through *Z*-AB is much lower than that through *Z*-AB-C2. It leads to the result that the on-off ratios of ABs are greatly higher than that of AB-C2s, and the shapes for on-off ratio curves of ABs and AB-C2 are totally different (Fig. 8A).

The big conductance gap between *E*/*Z* isomers of AB also proves the excellent photoswitching characteristics of ABs (Fig. 8B). Experiments have testified that the AB-C2s can overcome many defects of ABs such as low photochemical fatigue, almost the same wavelength that the two isomers absorb for iso merisation, and so on. However, there are many tasks to be completed in improving its photoswitching performance, especially the on-off ratio.

2) Spatial Distributions of HOMO and LUMO Orbitals

The effects of *E*/*Z* structures and connections on electronic structures are analyzed by HOMO, LUMO and HLG in Fig. S3. The electron of *E*-AB can inject into LUMO from electrode or hop into electrode from HOMO more easily than that of *Z*-AB. The similar conclusion can also get from the HLG-*V* curves of *E*/*Z* isomers of AB-C2. The results in Fig. S4 also give an excellent explanation to the electron transport in *E*/*Z* isomers of AB and AB-C2 and their different photoswitching performance by comparing the transmission spectra with PDOS.

In Fig. 9, here we emphasize on the spatial distributions of HOMO-1, HOMO, LUMO and LUMO+1 orbitals of *E*/*Z* isomers of AB and AB-C2 at 1.0 V. The MOs are projected onto the molecule from the junctions, as a result, the effect of Au electrodes is also included. It is obvious that the π-overlapping and the π-electron conjugations are reduced by switching from the *E*-isomers of AB and AB-C2 to the *Z*-isomers of AB and AB-C2. The bridge C atoms in AB-C2 hinder the π-overlapping and the π-electron conjugations, so they hinder the electron transport in AB-C2.

2.4 Fulgimides and Diarylethenes

1) Electron Transport Properties

Among the many classes of photochromic compounds, diarylethenes and fulgimides have generated the greatest interest, because they meet many of the aforementioned requirements for photoswitching units that are achieved by chemical transformations from electrocyclic ring closure of the hexatriene

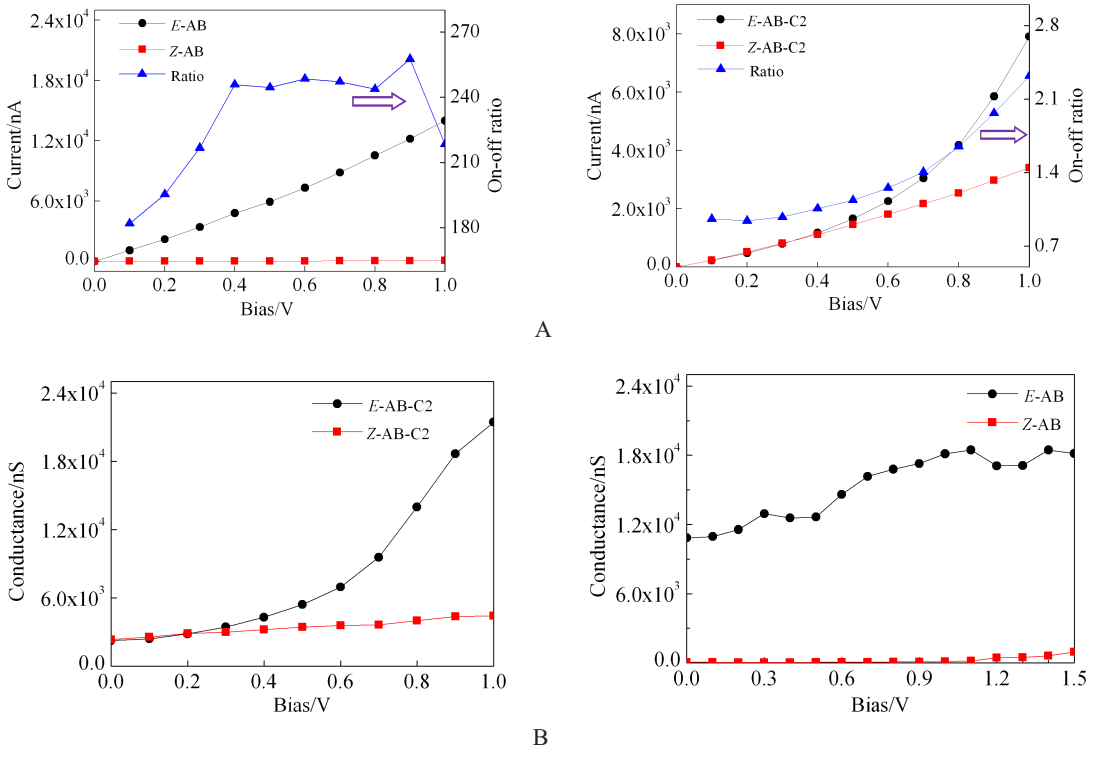

Fig. 8 A. The *I-V* and on-off ratio curves as function of the bias; B. The conductance-bias curves of *E*/*Z* isomers of ABs and AB-C2s (the bias changes from 0.0 V to 1.0 V)

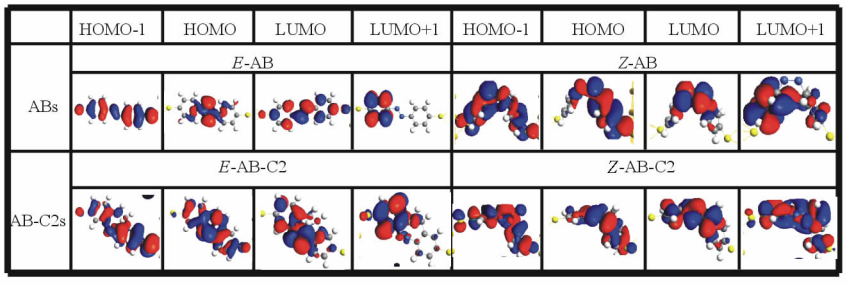

Fig. 9 Spatial distributions of HOMO-1, HOMO, LUMO and LUMO+1 at the bias of 1.0 V, including *E*/*Z* isomers of ABs and AB-C2s

backbone to cyclohexadiene under photoexcitation. Previous studies have demonstrated that fulgides are unstable in hydrolytic solvents relative to the corresponding fulgimides (FM). In FMs, the anhydride moiety of the fulgide is replaced with an imide moiety. FM derivatives are considered as a series of good switching materials because they present excellent switching reversibility, thermal stability of the differ ent isomers and resistance to fatigue in solu tion. Diarylethene (DT) containing heterocyclic aromatic group is also a most promising molecular switch material in the actual device as it has a good thermal stability, strong light sensitivity and high fatigue resistance characteristics. The opened-ring DT (opened-DT) transforms into closed-ring DT (closed-DT) after absorbing UV light and reversible reaction happens after absorbing VIS-light. However, the reversible transformation only occurs in solution. When DT is connected to Au electrode, the closed-DT can transform to the opened-DT but the reversible cannot happen as the high coupling between DT molecule and Au electrode hinders the cy clization reaction. Therefore, different

functional groups are added onto DTs to change the coupling degree and to make the reversible reaction occur. It is found that adding cyclization or replacing H in DT with F can achieve the two-way switch[59-61].

First, we analyze the photoswitching characteristics of FMs and DTs. The calculated *I-V* characteristics of the molecular switch at bias up to 1.0 V are plotted in Figure 10. One can see that the current curves of FMs and DTs are a little different, in which the current through closed-FM has a peak at 0.6 V and then drops sharply, but both the currents through closed and opened forms of DT increase sharply and then their increasing trends slow down at high bias. However, the current through the opened form of FM is strongly suppressed over the entire bias range, while the current through the closed form is evidently larger than that through the opened forms of FM and DT. As a result, their on-off ratios are different in which the max ratio of FMs is 103.8 at 0.5 V that is nearly 10 times to that of DTs at 0.1 V. It is attributed to the huge difference between the currents through the opened form of FM and DT. This shows that the electronic structure of molecule is of crucial importance in determining the low bias transport when nanoscale electrodes are used.

Meanwhile, the conductance curves of FMs and DTs are different, which is resulted from their different current curves (Fig. 10B). The conductance of closed-FM has a peak at 0.4 V and then decreases with the bias, but the conductance of opened-FM increases lowly in the entire bias range similar to its current. The conductance of closed-DT keeps decreasing as the bias increases whereas the conductance of opened-DT has a peak at the bias of 0.5 V.

2) Spatial Distributions of HOMO and LUMO Orbitals

The results of HOMO, LUMO and HLG are shown in Fig. S5. The excellent conjugation of closed-FM narrows the energy gap, thus, it determines the on/off states of FMs. The LUMO level of closed-DT provides a channel for electron transport of closed-DT more efficiently. As a result, the con

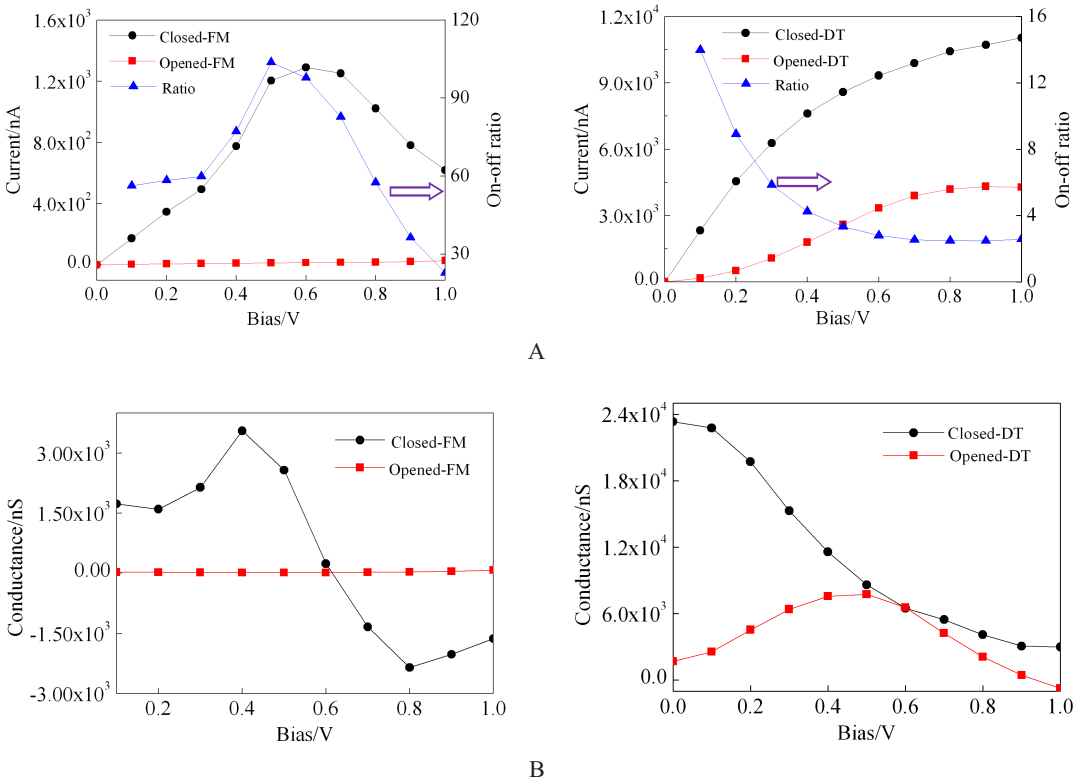

Fig. 10 A. The *I-V* and on-off ratio curves as function of the bias; B. The conductance-bias curves of FMs and DTs with closed and opened-ring junctions (the bias changes from 0.0 V to 1.0 V)

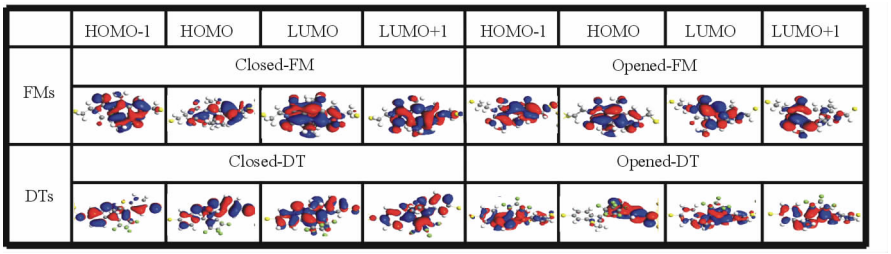

Fig. 11 Spatial distributions of HOMO-1, HOMO, LUMO and LUMO+1 at the bias of 1.0 V, including FMs and DTs with closed and opened-ring junctions

ductance and current of closed-DT are a little higher than those of opened-DT. The transmission and PDOS spectra in Fig. S6 help us explore the origin of the photoswitchable characteristics of these two systems.

Another static feature of the molecular junction is the spatial distribution presented in Fig. 11, which partially presents the mobility of the π-electron in the molecular switch system. The LUMO and LUMO+1 of FM and DT in closed ring forms are both delocalized orbtials which provide the main channel leading to low barrier for electron transport. However, the HOMO-1 and HOMO are both localized orbitals for the opened ring form, which cannot provide good transport channel, as the opened ring weakens molecular conjugation in the switch systems.

3 Conclusions

In summary, we designed a series of optical molecular switches based on different conformational transformations under photoexcitation and investigated the electron transportation behaviors of the molec ular wires using the DFT combined the NEGF formalism. We have demonstrated that every photochromic molecule mentioned here has two discrete current on/off states. From the systematic investigations, we suggested that photoswitching units with the same conformational transformation usually have similar current on/off states. Furthermore, it is impor tant that the spatial distribution of frontier molecular orbitals on molecules deeply influences the electron transfer efficiency and the bias also affects the on/off ratios.

Supporting Information Available

The supporti ng information is available free of charge via the internet at http://electrochem.xmu.edu.cn.

References:

[1] Feringa B L. In control of motion: From molecular switches to molecular motors[J]. Accounts of Chemical Research, 2001, 34(6): 504-513.

[2] Irie M. Diarylethenes for memories and switches [J]. Chemical Reviews, 2000, 100(5): 1685-1716.

[3] Tian H, Yang S J. Recent progresses on diarylethene based photochromic switches[J]. Chemical Society Reviews, 2004, 33(2): 85-97.

[4] Jin L M, Li Y N, Ma J, et al. Synthesis of novel thermally reversible photochromic axially chiral spirooxazines [J]. Organic Letters, 2010, 12(15): 3552-3555.

[5] Dugave C, Demange L. Cis-trans isomerization of organic molecules and biomolecules: Implications and applications [J]. Chemical Reviews, 2003, 103(7): 2475-2532.

[6] Delaire J A, Nakatani K. Linear and nonlinear optical properties of photochromic molecules and materials [J]. Chemical Reviews, 2000, 100(5): 1817-1845.

[7] Renth F, Siewertsen R, Temp F. Enhanced photoswitching and ultrafast dynamics in structurally modified photochromic fulgides[J]. International Reviews in Physical Chemistry, 2013, 32(1): 1-38.

[8] Collier C P, Mattersteig G, Wong E W, et al. A [2]catenane-based solid state electronically reconfigurable switch [J]. Science, 2000, 289(18): 1172-1175.

[9] Zheng C H, Pu S Z, Pang Z Y, et al. Syntheses and photochromism of new isomeric diarylethenes bearing an indole moiety[J]. Dyes and Pigments, 2013, 98(3): 565-574.

[10] Heshmat B, Pahlevaninezhad H, Darcie T E. Optical efficiency enhancement methods for terahertz receiving photoconductive switches[J]. Optics & Laser Technology, 2013, 54: 297-302.

[11] Coelho P J, Castro M C R, Raposo M M M. Reversible trans-cis photoisomerization of new pyrrolidene heterocyclic imines[J]. Journal of Photochemistry and Photobiology A: Chemistry, 2013, 259: 59-65.

[12] Dulic D, van der Molen S J, Kudernac T, et al. One-way optoelectronic switching of photochromic molecules on gold[J]. Physical Review Letters, 2003, 91(20): 207402-1-4.

[13] Schenderlein H, Voss A, Stark R W, et al. Preparation and characterization of light-switchable polymer networks attached to solid substrates[J]. Langmuir, 2013, 29 (14): 4525-4534.

[14] Zhao L Y, Hou Q F, Sui D, et al. Multistate/multifunctional switches based on photochromic Schiff base [J]. Spectrochimica Acta Part A-Molecular and Biomolecular Spectroscopy, 2007, 67(3/4): 1120-1125.

[15] Plaquet A, Guillaume M, Champagne B, et al. In silico optimization of merocyanine-spiropyran compounds as second-order nonlinear optical molecular switches [J]. Physical Chemistry Chemical Physics, 2008, 10 (41): 6223-6232.

[16] Jankowska J, Rode M F, Sadlej J, et al. Photophysics of schiff bases: Theoretical study of sal icylidene methylamine[J]. ChemPhysChem, 2012, 13(18): 4287-4294.

[17] Grzegorzek J, Filarowski A, Mielke Z. The photoinduced isomerization and its implication in the photo-dynamical processes in two simple Schiff bases isolated in solid argon[J]. Physical Chemistry Chemical Physics, 2011, 13 (37): 16596-16605.

[18] Maurer R J, Reuter K. Assessing computationally efficient isomerization dynamics: Delta SCF density-functional theory study of azobenzene molecular switching[J]. The Journal of Chemical Physics, 2011, 135(22): 224303-1-10.

[19] Satzger H, Root C, Braun M. Excited-state dynamics of trans- and cis-azobenzene after UV excitation in the ππ* band[J]. The Journal of Physical Chemistry A, 2004, 108 (30): 6265-6271.

[20] Perrier A, Maurel F, Jacquemin D. Single molecule multiphotochromism with diarylethenes [J]. Accounts of Chemical Research, 2012, 45(8): 1173-1182.

[21] Taguchi M, Nakagawa T, Nakashima T, et al. Photochromic and fluorescence switching properties of oxidized triangle terarylenes in solution and in amorphous solid states [J]. Journal of Materials Chemistry, 2011, 21 (43): 17425-17432.

[22] Miskolczy S, Biczok L. Photochromism of a merocyanine dye bound to sulfonatocalixarenes: Effect of pH and the size of macrocycle on the kinetics [J]. The Journal of Physical Chemistry B, 2013, 117(2): 648-653.

[23] Villeneuve C H, Michalik F, Chazalviel J N, et al. Quantitative IR readout of fulgimide mono layer switching on Si(111) surfaces [J]. Advanced Materials, 2013, 25(3): 416-421.

[24] Jin L M, Li Y N, Ma J, et al. Synthesis of novel thermally reversible photochromic axially chiral spirooxazines [J]. Organic Letters, 2010, 12(15): 3552-3555.

[25] Berkovic G, Krongauz V, Weiss V. Spiropyrans and spirooxazines for memories and switches[J]. Chemical Reviews, 2000, 100(5): 1741-1753.

[26] Hadjoudis E, Rontoyianni A, Ambroziak K, et al. Photochromism and thermochromism of solid trans-N,N′-bis-(salicylidene)-1,2-cyclohexanediamines and trans-N, N′-bis-(2-hydroxy-naphylidene)-1,2-cyclohexane-diamine [J]. Journal of Photochemistry and Photobiology A: Chemistry, 2004, 162(2/3): 521-530.

[27] Feringa B L. Molecular switches[M]. Weinheim: Wiley-VCH Verlag GmbH, 2001: 281.

[28] Feringa B L. Molecular switches[M]. Weinheim: Wiley-VCH Verlag GmbH, 2001: 37.

[29] Seminario J M, Politzer P. Molecular density functional theory a tool for chemistry[M]. Amsterdam: Elesvier B V, 1995: 173-175.

[30] Frisch M J, Trucks G W, Schlege H B, et al. GAUSSIAN 03[EB]. Gaussian, Inc. Wallingford CT, 2004.

[31] Lee C T, Yang W T, Parr R G. Development of the colle-salvetti correlation-energy formula into a functional of the electron density[J]. Physical Review B, 1988, 37 (2): 785-789.

[32] Salzner U, Lagowski J B, Pickup P G, et al. Design of low band gap polymers employing density functional theory-hybrid functionals ameliorate band gap problem [J]. Journal of Computational Chemistry, 1997, 18(15): 1943-1953.

[33] Hay P J, Wadt W R. *Ab initio* effective core potentials for molecular calculations. Potentials for the transition metal atoms Sc to Hg[J]. The Journal of Chemical Physics, 1985, 82(1): 270-284.

[34] Wadt W R, Hay P J. *Ab initio* effective core potentials for molecular calculations. Potentials for main group elements Na to Bi[J]. Journal of Chemical Physics, 1985, 82 (1): 284-298.

[35] Schaefer H F. Modern theoretical chemistry[M]. New York: Plenum Press, 1976: 1-28.

[36] Gronbeck H, Curioni A, Andreoni W. Thiols and disulfides on the Au(111) surface: The headgroup-gold interaction [J]. Journal of the American Chemical Society,

2000, 122(16): 3839-3842.

[37] Yin X, Liu H M, Zhao J W. Electronic transportation through asymmetrically substituted oli go (phenylene ethynylene)s: Studied by first principles nonequilibrium Green's function formalism[J]. Journal of Chemical Physics, 2006, 125(9): 094711-1-6.

[38] Liu H M, Li P, Zhao J W, et al. Theoretical investigation on molecular rectification on the basis of asymmetric substitution and proton transfer reaction[J]. Journal of Chemical Physics, 2008, 129(22): 224704-1-6.

[39] Stokbro K, Taylor J, Brandbyge M. Do Aviram-Ratner diodes rectify?[J]. Journal of the American Chemical Society, 2003, 125(13): 3674-3675.

[40] Zhao P, Liu D S, Wang P J, et al. First-principles study of the electronic transport properties of the anthraquinone-based molecular switch [J]. Physica B-Condensed Matter, 2011, 406(4): 895-898.

[41] Fan Z Q, Zhang Z H, Ming Q, et al. First-principles study of repeated current switching in a bimolecular device[J]. Computational Materials Science, 2012, 53(1): 294-297.

[42] Atomistix ToolKit, QuantumWise A/S[EB/OL]. www.quantumwise.com (access 2006).

[43] Yaliraki S N, Roitberg A E, Gonzalez C, et al. The injecting energy at molecule/metal interfaces: Implications for conductance of molecular junctions from an *ab initio* molecular description[J]. The Journal of Chemical Physics, 1999, 111(15): 6997-7002.

[44] Hall L E, Reimers J R, Hush N S, et al. Formalism, analytical model, and a priori Green's-function-based calculations of the current-voltage characteristics of molecular wires[J]. The Journal of Chemical Physics, 2000, 112(3): 1510-1521.

[45] Tomfohr J, Sankey O F. Theoretical analysis of electron transport through organic molecules[J]. The Journal of Chemical Physics, 2004, 120(3): 1542-1554.

[46] Zhao P, Liu D S, Wang P J, et al. First-principles study of the electronic transport properties of the an thraquinone-based molecular switch[J]. Journal of Physics: Condensed Matter, 2011, 406(4): 895-898.

[47] Zhao W K, Yang C L, Wang M S, et al. Effects of electrode orientation on the transport proper ties of pyridine-terminated dithienylethene light molecule switch under bias[J]. Solid State Communications, 2013, 153(1): 1-7.

[48] Datta S. Electronic transport in mesoscopic systems[M]. New York: Cambrideg University Press, 1995.

[49] Castro P J, Gomez I, Cossi M, et al. Computational study of the mechanism of the photochemical and thermal ring-opening/closure reactions and solvent dependence in spirooxazines[J]. The Journal of Physical Chemistry A, 2012, 116(31): 8148-8158.

[50] Buttiker M. Four-terminal phase-coherent conductance [J]. Physical Review Letters, 1986, 57(14): 1761-1764.

[51] Meir Y, Wingreen N S. Landauer formula for the current through an interacting electron region[J]. Physical Review Letters, 1992, 68(16): 2512-2515.

[52] Yin X, Li Y W, Zhang Y, et al. Theoretical analysis of geometry-correlated conductivity of molecular wire [J]. Chemical Physics Letters, 2006, 422(1/3): 111-116.

[53] Seminario J M, Zacarias A G, Tour J M. Theoretical study of a molecular resonant tunneling diode[J]. Journal of the American Chemical Society, 2000, 122(13): 3015-3020.

[54] Hanif M, Lu P, Li M, et al. Synthesis, characterization, electrochemistry and optical properties of a novel phenanthrenequinonealt-dialkylfluorene conjugated copolymer [J]. Polymer International, 2007, 56(12): 1507-1513.

[55] Knyazhansky M I, Metelitsa A V, Kletskii M E, et al. The structural transformations and photo-induced processes in salicylidene alkylimines[J]. Journal of Molecular Structure, 2000, 526: 65-79.

[56] Zhou Y H, Yuan L Z, Zheng X H. *Ab initio* study of the transport properties of a light-driven switching molecule azobenzene substituent[J]. Computational Materials Science, 2012, 61: 145-149.

[57] Böckmann M, Doltsinis N L, Marx D. Enhanced photoswitching of bridged azobenzene studied by nonadiabatic *ab initio* simulation[J]. Journal of Chemical Physics, 2012, 137(22): 22A505-1-10.

[58] Siewertsen R, Sch?nborn J B, Hartke B, et al. Superior *Z-E* and *E-Z* photoswitching dynamics of dihydrodibenzodiazocine, a bridged azobenzene, by $S_1(n\pi^*)$ excitation at k = 387 and 490 nm [J]. Physical Chemistry Chemical Physics, 2011, 13(3): 1054-1063.

[59] Xia C J, Liu D S, Liu H C. Phenylazoimidazole as a possible optical molecular switch: An *ab initio* study[J]. Optik, 2012, 123(14): 1307-1310.

[60] Wolak M A, Thomas C J, Gillespie N B, et al. Tuning the optical properties of fluorinated indolylfulgimides [J]. Journal of Organic Chemistry, 2003, 68(2): 319-326.

[61] Zhao P, Wang P J, Zhang Z, et al. Electronic transport properties of a diarylethene-based molecular switch with single-walled carbon nanotube elec trodes: The effect of chirality[J]. Solid State Communications, 2009, 149 (23/24): 928-931.

结构转变方式对光致变色分子开关输运性能影响的从头计算研究

贺园园,赵健伟*

(南京大学 化学化工学院, 生命分析化学国家重点实验室, 江苏 南京 210008)

摘要: 采用密度泛函理论方法系统地研究了由不同结构转变方式引发的一系列光致变色分子在用于分子开关时的电子输运性质. 对各种分子结构转变前后的最高占据轨道(HOMO)与最低空轨道(LUMO)的能级间隙(HLG)、前线轨道的空间分布、电子透射谱和投影电子态密度(PDOS)谱进行了计算和讨论. 结果表明,相似的结构转变方式通常造成分子具有相似的电流开关性质, 这与分子的共轭程度又有一定的关系. 比较各种分子的电流开关比后发现偶氮苯结构单元具有最大的电流开关比.

关键词: 结构转变方式;光致变色;电子传递;电流开关比;分子轨道